

Supporting Information

Supporting Information

(20 pages including the cover page)

Inter-Ligand Electronic Coupling Mediated Through Dimetal Bridge: Dependence on Metal Ions and Ancillary Ligands

Moumita Majumdar, Sayantani Saha, Indranil Dutta, Arup Sinha and Jitendra. K. Bera*

Department of Chemistry, Indian Institute of Technology Kanpur, Kanpur 208016, India

E-mail: jbera@iitk.ac.in

Contents

	Page No.
Experimental Section	S2–S9
X–Ray Data Collection and Refinement	S9–S12
Table S8. Chemical shift values for H _a protons	S12
Figure S1. Cyclic voltammetry of (a) L ¹ and (b) L ²	S13
Figure S2. Cyclic voltammetry of 6A	S13
Figure S3–S11. UV–Visible absorption spectra of 1 , 2 , 3 , 3A , 4 , 5 , 5A , 6 , 6A	S13–S16
Figure S12. UV–vis changes monitored (with time) at four potentials for 3A	S17
Figure S13. EPR spectrum for 1 in CH ₃ CN	S17
Scheme S10. Interaction between metal and the acetate orbitals	S18
Theoretical Study	S18
References	S18–S20

Experimental Section

General Procedures. All reactions with metal complexes were carried out under an atmosphere of purified nitrogen using standard Schlenk–vessel and vacuum line techniques. Glasswares were flame–dried under vacuum. The crystallized compounds were powdered, washed several times with dry petroleum ether, and dried in vacuum for at least 48 h prior to elemental analyses. NMR spectra were obtained on JEOL JNM–LA 500 MHz spectrometer. ^1H NMR chemical shifts were referenced to the residual hydrogen signal of the deuterated solvents. The chemical shift is given as dimensionless δ values and the frequency is referenced relative to TMS for ^1H and ^{13}C NMR. Elemental analyses were performed on a Thermoquest EA1110 CHNS/O analyzer. Infrared spectra were recorded in the range 4000–400 cm^{-1} on a Vertex 70 Bruker spectrophotometer on KBr pellets. ESI–MS were recorded on a Waters Micromass Quattro Micro triple–quadrupole mass spectrometer. ESI–MS of compounds were recorded in acetonitrile. Cyclic voltammetric studies were performed on a BAS Epsilon electrochemical workstation in acetonitrile with 0.1 M tetra–*n*–butylammonium hexafluorophosphate (TBAPF₆) as the supporting electrolyte. The working electrodes were BAS Pt disk electrode and glassy carbon electrode, the reference electrode was Ag/AgCl and the auxiliary electrode was a Pt wire. The ferrocene/ferrocenium couple occurs at $E_{1/2} = +0.51$ (70) V versus Ag/AgCl under the same experimental conditions. The potentials are reported in volts (V); the ΔE ($E_{\text{p,a}} - E_{\text{p,c}}$) values are in millivolts (mV) at a scan rate of 100 mVs^{-1} . A platinum wire–gauze working electrode was used in coulometric experiments. Optically transparent Pt gauze electrode was used as working electrode. Pt wire was used as counter electrode and Ag/AgCl as reference electrode. Electronic absorptions were measured on a Lambda–20 Perkin–Elmer spectrophotometer. Ultraviolet–visible spectroelectrochemical experiments were performed using Thin Layer Quartz Crystal Spectroelectrochemical cell. The quartz cuvette has 1 cm path length. UV–vis absorption scans were recorded on an Ocean Optics USB4000 (BASi, USA) UV–vis spectrometer in dry acetonitrile. EPR spectra were recorded on a Bruker EMX X–band spectrometer at 120 K.

Materials. All manipulations were carried out under an inert atmosphere with the use of standard Schlenk–line techniques. Glass wares were flame–dried under vacuum prior to use. Solvents were dried by conventional methods, distilled over nitrogen and deoxygenated prior to use. The reagents Mo(CO)₆, HBF₄ (51–57% in diethyl ether), Et₃OB₄ (1 M in CH₂Cl₂) and Cu metal were purchased from Aldrich. RuCl₃.xH₂O (39% Ru) and RhCl₃.xH₂O (40%

Supporting Information

Rh) were purchased from Arora Matheys, Kolkata. Trifluoromethane sulphonic acid was purchased from Spectrochem, India and Cu(ClO₄)₂.6H₂O was purchased from SD Fine-Chem Limited, India. The starting materials [Mo₂(OAc)₄]¹, *cis*-[Mo₂(OAc)₂(CH₃CN)₆][BF₄]₂², [Mo₂(CH₃CN)₁₀][BF₄]₄³, Ru₂(OAc)₄Cl⁴, [Ru₂(CO)₄(CH₃CN)₆][OTf]₂⁵, [Rh₂(OAc)₄]⁶, [Rh₂(OAc)₂(CH₃CN)₆][BF₄]₂⁷, [Cu(CH₃CN)₄][ClO₄]⁸ were synthesized according to the literature procedures. The ligands 2-(2-pyrazinyl)-1,8-naphthyridine (L¹) and 2-(2-thiazolyl)-1,8-Naphthyridine (L²) were prepared by the Friedlander condensation of 2-aminonicotinaldehyde with corresponding acyl derivatives.⁹

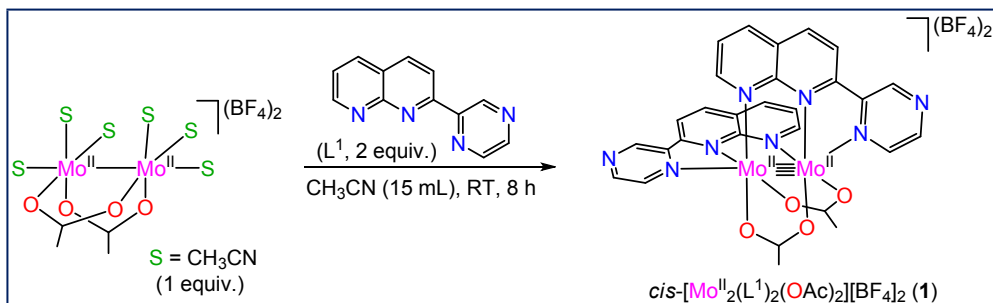
Synthesis and Characterization

Synthesis of L¹. A stirred solution of 2-acetylpyrazine (520 mg, 4.26 mmol) and 2-aminonicotinaldehyde (500 mg, 4.10 mmol) was heated to 60°C. Methanolic KOH (560 mg, 10 mmol) solution was added to the reaction mixture and it was refluxed overnight. The solvent was evaporated under reduced pressure. The crude solid was purified by column chromatography (silica gel, EtOAc/Hexane: 40/60) to afford white solid. Yield: 724 mg (85%). ¹H NMR (500 MHz, CDCl₃, 292 K): 10.05 (s, 1H), 9.18 (q, J = 2.3 Hz, 1H), 8.66–8.68 (m, 3H), 8.36 (d, J = 8 Hz, 1H), 8.25 (dd, J = 6.3 Hz, J = 1.75 Hz, 1H), 7.54 (q, J= 4.55 Hz, 1H). ¹³C NMR (125 MHz, CDCl₃, 292 K): 157.5, 155.7, 154.3, 150.4, 145.3, 144.7, 143.5, 138.3, 137.0, 122.2, 122.6, 120.0. ESI-MS, m/z: 209.0822, [M + H]⁺. Anal. Calcd. for C₁₂H₈N₄: C, 69.22; H, 3.87; N, 26.91. Found: C, 70.10; H, 3.68; N, 27.40.

Synthesis of L². The reaction of 2-acetylthiazole (541 mg, 4.26 mmol), 2-aminonicotinaldehyde (500 mg, 4.10 mmol) and methanolic KOH (560 mg, 10 mmol) solution was carried out following a similar procedure described for the synthesis of L¹. The crude solid was purified by column chromatography (silica gel, EtOAc/Hexane: 40/60) to afford whitish pink solid. Yield: 715 mg (82%). ¹H NMR (500 MHz, CDCl₃, 292 K): 9.13 (q, J = 2 Hz, 1H), 8.45 (d, J = 8.6 Hz, 1H), 8.28 (d, J = 8Hz, 1H), 8.20 (dd, J = 6.3 Hz, J = 2.3 Hz, 1H), 7.99 (d, J = 2.85 Hz, 1H), 7.55 (d, J = 4.4 Hz, 1H), 7.49 (q, J = 4 Hz, 1H). ¹³C NMR (125 MHz, CDCl₃, 292 K): 168.8, 155.6, 154.3, 154.2, 144.3, 138.2, 136.9, 123.3, 122.4, 118.9. ESI-MS, m/z: 214.0415, [M + H]⁺. Anal. Calcd. for C₁₂H₈N₄: C, 61.95; H, 3.31; N, 19.70. Found: C, 62.15; H, 3.15; N, 20.40.

Synthesis of *cis*-[Mo₂L¹₂(OAc)₂][BF₄]₂ (1**)**.

Ligand L¹ (50 mg, 0.24 mmol) was added to an acetonitrile solution (15 mL) of [Mo₂(OAc)₂(CH₃CN)₆][BF₄]₂ (88 mg, 0.12 mmol). The mixture was stirred for 8 h which resulted a color change from light pink to dark green. After the completion of the reaction, the solution was concentrated under vacuum and 15 mL of toluene was added with stirring to induce precipitation. The resulting solid residue was washed with diethyl ether (3 × 10 mL) and dried in vacuum. X-ray quality crystals were grown by layering diethyl ether onto a saturated acetonitrile solution of **1** inside an 8 mm o.d. vacuum-sealed glass tube. Yield: 92 mg (85%). ¹H NMR (500 MHz, DMSO-d₆, 292 K): δ 9.72 (s, 2H), 9.14 (q, J = 2.3 Hz, 2H), 8.80 (d, J = 13.75 Hz, 4H), 8.67 (d, J = 8.6 Hz, 2H), 8.57 (m, 4H), 7.71–7.68 (m, 2H), 2.62 (br, 6H). ¹³C NMR (125 MHz, DMSO-d₆, 292K): δ 172.5, 157.3, 154.9, 154.6, 150.2, 146.4, 144.8, 143.9, 140.1, 138.9, 123.7, 120.1, 24.3, 21.6. ESI-MS, m/z: 362.9909, [M – 2BF₄]²⁺. IR (KBr, cm⁻¹): ν(OAc⁻); 1605, 1436, ν(BF₄⁻); 1052. UV-Vis [CH₃CN; λ_{max}, nm (ε, dm³ mol⁻¹ cm⁻¹)]: 241 (6.90 × 10⁴), 285 (4.83 × 10⁴), 296 (4.81 × 10⁴), 318 (6.62 × 10⁴), 330 (6.65 × 10⁴), 355(sh), 455 (0.52 × 10⁴). Anal. Calcd. for C₂₈H₂₂N₈O₄B₂F₈Mo₂: C, 37.37; H, 2.46; N, 12.45. Found: C, 36.83; H, 2.54; N, 12.47.

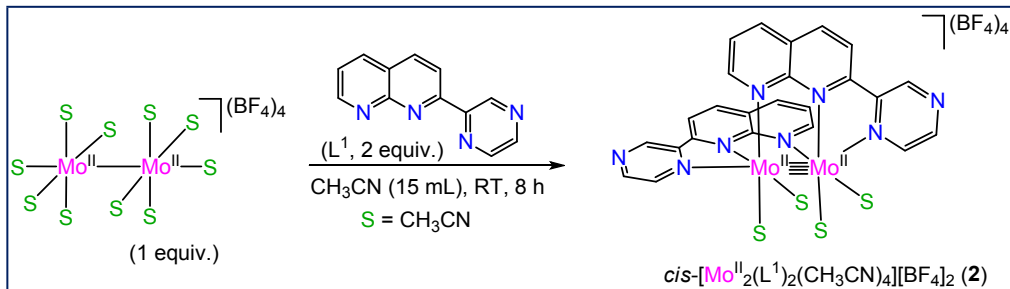


Scheme S1 Synthesis of compound **1**.

Synthesis of *cis*-[Mo₂L¹₂(CH₃CN)₄][BF₄]₄ (2**)**.

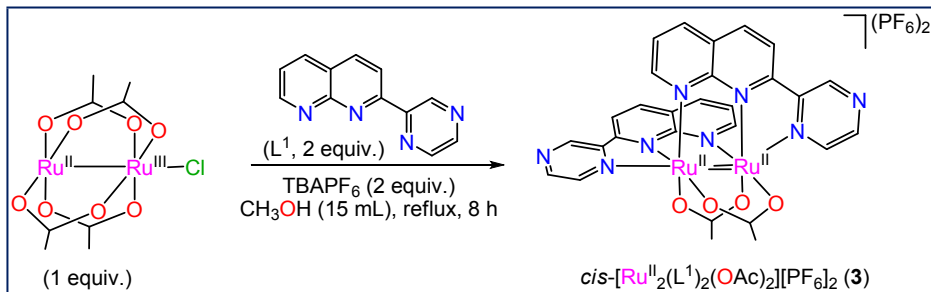
The reaction of ligand L¹ (50 mg, 0.24 mmol) and [Mo₂(CH₃CN)₁₀][BF₄]₄ (114 mg, 0.12 mmol) was carried out following a similar procedure described for the synthesis of complex **1**. The color of the solution changed from pink to dark green upon addition of L¹. To obtain pure crystalline compound, 10 mL of diethyl ether was layered onto a saturated acetonitrile solution of **2** in a schlenk tube. Yield: 112 mg (84%). ¹H NMR (500 MHz, DMSO-d₆, 292 K): δ 9.72 (s, 2H), 9.21 (s, 2H), 8.82 (d, J = 11.45 Hz, 4H), 8.72 (m, 4H), 8.64 (d, J = 9.15 Hz, 2H), 7.79 (dd, J = 4 Hz, J = 3.6 Hz, 2H), 2.46 (s, 6H), 2.03 (s, 6H). ¹³C NMR (125 MHz, DMSO-d₆, 292K): δ 172.5, 157.9, 153.6, 149.9, 146.6, 144.9, 143.9, 140.9, 140.2, 123.8, 120.8, 118.6, 21.6. ESI-MS, m/z: 362.9979, [M – 3CH₃CN – 2BF₄ + 6H₂O]²⁺. IR (KBr, cm⁻¹): ν(CN): 2922; ν(BF₄⁻): 1055. UV-Vis [CH₃CN; λ_{max}, nm (ε, dm³ mol⁻¹ cm⁻¹)]: 231 (5.36 × 10⁴), 283 (3.06 × 10⁴), 324

(2.92×10^4) , 363 (sh), 452 (0.31×10^4). Anal. Calcd. for $(C_{32}H_{19}N_9B_4F_{16}Mo_2)(H_2O)_4$: C, 29.08; H, 2.54; N, 11.74. Found: C, 28.45; H, 2.53; N, 11.16.



Scheme S2 Synthesis of compound 2.

Synthesis of *cis*–[Ru^{II}₂(L¹)₂(OAc)₂][PF₆]₂ (3). Ligand L¹ (50 mg, 0.24 mmol) was added to a methanolic solution (15 mL) of [Ru₂(OAc)₄Cl] (57 mg, 0.12 mmol) and TBAPF₆ (93 mg, 0.24 mmol). The mixture was refluxed overnight and initial dark brown color of the solution turned to dark green. Upon completion, the reaction was cooled and the solution was concentrated under vacuum and 15 mL of toluene was added with stirring to induce precipitation. The solid residue was washed with diethyl ether (3 × 10 mL) and dried in vacuum. To obtain pure crystalline compound, 10 mL of diethyl ether was layered onto a saturated acetonitrile solution of 3 in a schlenk tube. Yield: 110 mg (90%). ESI–MS, m/z: 882.9498, [M – PF₆]⁺; 368.9861 [M – 2PF₆]²⁺. IR (KBr, cm^{−1}): v(OAc[−]); 1605, 1438, v(PF₆[−]); 839. UV–Vis [CH₃CN; λ_{max}, nm (ε, dm³ mol^{−1} cm^{−1})]: 243 (3.35 × 10⁴), 265 (sh), 335 (6.76 × 10⁴), 440 (1.47 × 10⁴), 650 (1.63 × 10⁴), 771 (1.32 × 10⁴). Anal. Calcd. for (C₂₈H₂₂N₈O₄P₂F₁₂Ru₂)(CH₃CN)(H₂O): C, 33.12; H, 2.50; N, 11.59. Found: C, 33.33; H, 2.61; N, 11.42.

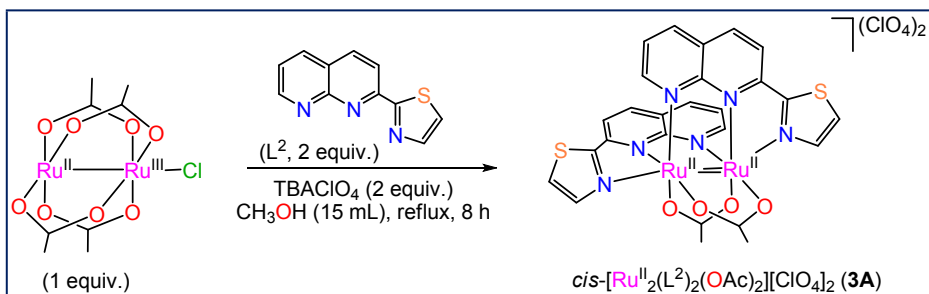


Scheme S3 Synthesis of compound 3.

Synthesis of *cis*–[Ru^{II}₂(L²)₂(OAc)₂][ClO₄]₂ (3A). The reaction of ligand L² (50 mg, 0.23 mmol), [Ru₂(OAc)₄Cl] (56 mg, 0.12 mmol) and TBAClO₄ (79 mg, 0.23 mmol) was carried out following a similar procedure described for the synthesis of complex 3. The solution

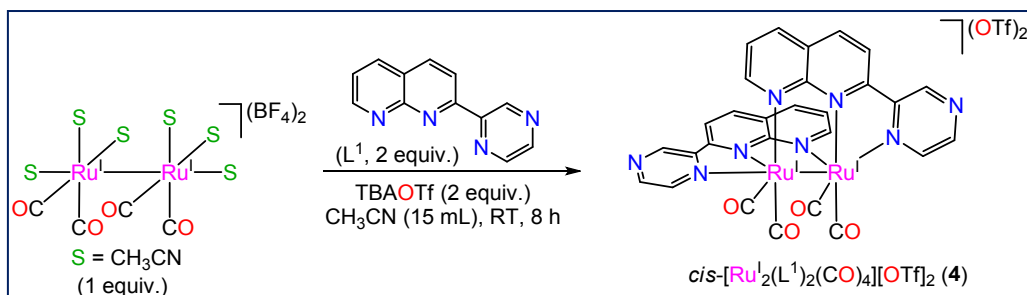
Supporting Information

color underwent color change from dark brown to dark blue upon addition of L². X-ray quality crystals were grown by layering diethyl ether onto a saturated acetonitrile solution of **3A** inside an 8 mm o.d. vacuum-sealed glass tube. Yield: 100 mg (90%). ESI-MS, m/z: 846.8575, [M – ClO₄]⁺; 373.9439 [M – 2ClO₄]²⁺. IR (KBr, cm⁻¹): ν(OAc⁻); 1601, 1432, ν(ClO₄⁻); 1088. UV-Vis [CH₃CN; λ_{max}, nm (ε, dm³ mol⁻¹ cm⁻¹)]: 256 (6.12 × 10⁴), 353 (12.97 × 10⁴), 465 (6.57 × 10⁴), 631 (1.74 × 10⁴), 779 (1.43 × 10⁴). Anal. Calcd. for (C₂₆H₂₀N₆O₁₂S₂Cl₂Ru₂)(H₂O)_{0.5}: C, 32.68; H, 2.22; N, 8.79. Found: C, 32.10; H, 2.29; N, 8.97.



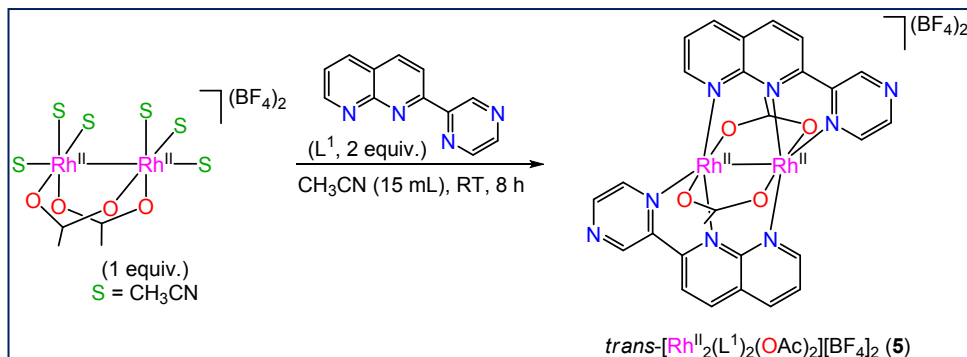
Scheme S4 Synthesis of compound **3A**.

Synthesis of cis-[Ru^I₂(L¹)₂(CO)₄][OTf]₂ (4). The reaction of ligand L¹ (50 mg, 0.24 mmol), [Ru₂(CO)₄(CH₃CN)₆][BF₄]₂ (88 mg, 0.12 mmol) and TBAOTf (94 mg, 0.24 mmol) was carried out following a similar procedure described for the synthesis of complex **1**. X-ray quality crystals were grown by layering diethyl ether onto a saturated acetonitrile solution of **4** inside an 8 mm o.d. vacuum-sealed glass tube. Yield: 108 mg (88%). ¹H NMR (500 MHz, DMSO-d₆, 292 K): δ 10.16 (s, 2H), 9.59 (q, J = 2.85 Hz, 2H), 9.38 (d, J = 3.45 Hz, 2H), 9.02 (dd, J = 14.3 Hz, J = 9.15, 4H), 8.77 (m, 4H), 7.75–7.72 (m, 2H). ¹³C NMR (125 MHz, DMSO-d₆, 292 K): δ 205.2, 199.1, 161.1, 160.9, 155.9, 151.7, 149.4, 148.6, 147.7, 143.4, 143.1, 127.4, 126.5, 123.5. ESI-MS, m/z: 323.9765, [M – 3CO – 2OTf]²⁺; 337.9778 [M – 2CO – 2OTf]²⁺, 351.9748 [M – CO – 2OTf]²⁺, 365.9753 [M – 2OTf]²⁺. IR (KBr) data (cm⁻¹): ν(CO); 2050, 1975, ν(OTf): 1057. UV-Vis [CH₃CN; λ_{max}, nm (ε, dm³ mol⁻¹ cm⁻¹)]: 240 (5.27 × 10⁴), 281 (5.20 × 10⁴), 342 (4.62 × 10⁴), 357 (sh). Anal. Calcd. for (C₃₂H₁₆N₈O₁₀F₆S₂Ru₂)(CH₃CN)(H₂O)₂: C, 34.69; H, 2.09; N, 11.39. Found: C, 34.67; H, 2.08; N, 11.28.



Synthesis of *trans*-[Rh₂L¹₂(OAc)₂][BF₄]₂ (5**)**.

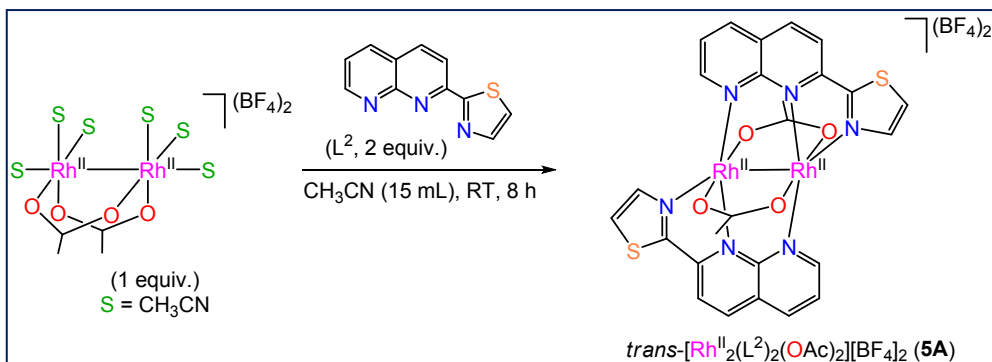
The reaction of ligand L¹ (50 mg, 0.24 mmol) and [Rh₂(OAc)₂(CH₃CN)₆][BF₄]₂ (90 mg, 0.12 mmol) was carried out following a similar procedure described for the synthesis of complex **1**. Pure crystalline compound was obtained by layering of diethyl ether onto a saturated acetonitrile solution of **5** in a schlenk tube. Yield: 90 mg (82%). ¹H NMR (500 MHz, CD₃CN, 292 K): δ 9.98 (br, 2H), 9.73–9.29 (m, 4H), 9.12 (br, 2H), 8.87–8.50 (m, 8H), 2.53 (br, 6H). ¹³C NMR (125 MHz, CD₃CN, 292K): δ 162.1, 162.6, 155.5, 151.5, 148.3, 143.8, 142.7, 141.8, 141.6, 127.7, 123.7, 120.9, 23.9, 23.2. ESI-MS, m/z: 369.9908, [M – 2BF₄]²⁺. IR (KBr, cm⁻¹): ν(OAc⁻); 1566, 1452, ν(BF₄⁻); 1060. UV-Vis [CH₃CN; λ_{max}, nm (ε, dm³ mol⁻¹ cm⁻¹)]: 240 (sh), 286 (4.02 × 10⁴), 317 (3.01 × 10⁴), 357 (sh), 474 (0.16 × 10⁴). Anal. Calcd. for (C₂₈H₂₂N₈O₄B₂F₈Rh₂)(H₂O)₄: C, 34.08; H, 3.07; N, 11.36. Found: C, 33.10; H, 3.09; N, 11.87.



Scheme S6 Synthesis of compound **5**.

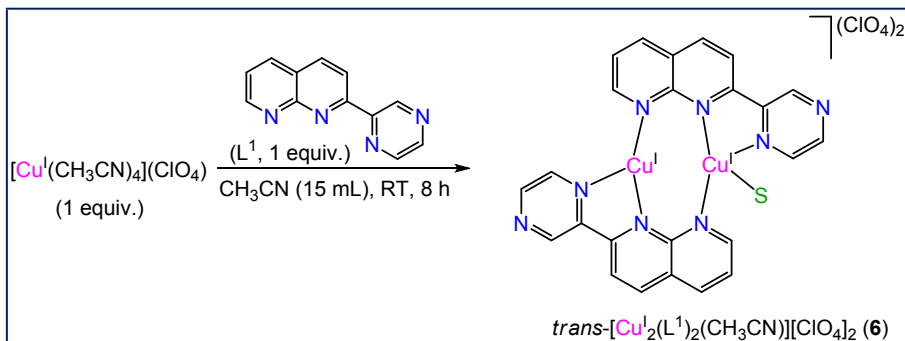
Synthesis of *trans*-[Rh₂L²₂(OAc)₂][BF₄]₂ (5A**)**.

The reaction of ligand L² (50 mg, 0.23 mmol) and [Rh₂(OAc)₂(CH₃CN)₆][BF₄]₂ (90 mg, 0.12 mmol) was carried out following a similar procedure described for the synthesis of complex **1**. X-ray quality crystals were grown by layering diethyl ether onto a saturated acetonitrile solution of **5A** inside an 8 mm o.d. vacuum-sealed glass tube. Yield: 92 mg (82%). ¹H NMR (500 MHz, CD₃CN, 292 K): 9.04 (br, 2H), 8.78–8.45 (m, 8H), 8.07 (s, 2H), 7.77 (br, 2H), 2.13 (br, 6H). ¹³C NMR (125 MHz, CD₃CN, 292K): δ 168.6, 155.5, 155.2, 153.9, 145.3, 144.0, 143.9, 140.2, 127.3, 125.1, 123.5, 24.6, 23.4. ESI-MS, m/z: 374.9531, [M – 2BF₄]²⁺. IR (KBr, cm⁻¹): ν(OAc⁻); 1577, 1428; ν(BF₄⁻); 1050. UV-Vis [CH₃CN; λ_{max}, nm (ε, dm³ mol⁻¹ cm⁻¹)]: 260 (3.73 × 10⁴), 285 (sh), 335 (3.37 × 10⁴), 375 (sh), 450 (0.15 × 10⁴). Anal. Calcd. for (C₂₆H₂₀N₆O₄S₂B₂F₈Rh₂)(CH₃CN)(H₂O): C, 31.85; H, 3.15; N, 9.29. Found: C, 30.37; H, 3.13; N, 9.78.



Scheme S7 Synthesis of compound **5A**.

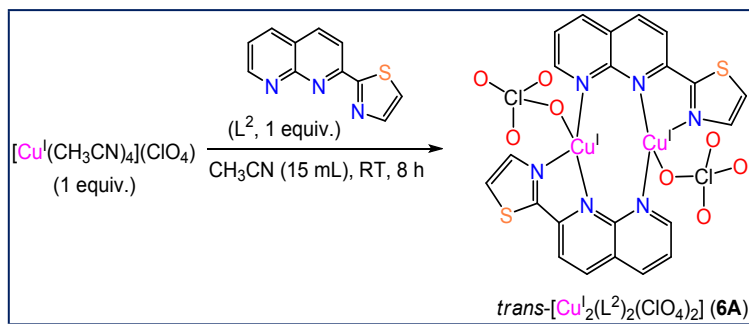
Synthesis of *trans*-[Cu₂L¹₂(CH₃CN)][ClO₄]₂ (6). The reaction of ligand L¹ (50 mg, 0.24 mmol) and [Cu(CH₃CN)₄](ClO₄) (98 mg, 0.24 mmol) was carried out following a similar procedure described for the synthesis of complex **1**. X-ray quality crystals were grown by layering diethyl ether onto a saturated acetonitrile solution of **6** inside an 8 mm o.d. Yield: 160 mg (85%). ¹H NMR (500 MHz, DMSO-d₆, 292 K): δ 10.19 (s, 2H), 9.19–9.02 (m, 10H), 8.91 (d, J = 9.2 Hz, 2H), 7.95 (s, 2H), 2.04 (s, 6H). ¹³C NMR (125 MHz, DMSO-d₆, 292 K): δ 169.0, 154.1, 156.4, 153.9, 149.8, 146.5, 146.2, 143.6, 141.7, 139.7, 126.3, 122.0, 118.6. ESI-MS: *m/z* 479.0782 [L¹₂Cu]⁺. IR (KBr, cm⁻¹): ν(ClO₄⁻); 1058. UV-Vis [CH₃CN; λ_{max}, nm (ε, dm³ mol⁻¹ cm⁻¹)]: 288 (7.27 × 10⁴), 322 (6.68 × 10⁴). Anal. Calcd. for (C₂₄H₁₆N₈Cl₂O₈Cu₂)(CH₃CN)₄: C, 42.78; H, 3.12; N, 18.59. Found: C, 44.34; H, 3.0; N, 18.08.



Scheme S8 Synthesis of compound **6**.

Synthesis of *trans*-[Cu₂L²₂][ClO₄]₂ (6A). The reaction of ligand L² (50 mg, 0.23 mmol) and [Cu(CH₃CN)₄](ClO₄) (94 mg, 0.23 mmol) was carried out following a similar procedure described for the synthesis of complex **1**. X-ray quality crystals were grown by layering diethyl ether onto a saturated acetonitrile solution of **6A** inside an 8 mm o.d. Yield: 140 mg (82%). ¹H NMR (500 MHz, DMSO-d₆, 292 K): δ 9.40 (br, 2H), 9.04 (d, J = 8 Hz, 2H), 8.93 (d, J = 6.85 Hz, 2H), 8.62 (d, J = 8.55 Hz, 2H), 8.49 (d, J = 19.45 Hz, 4H), 8.02 (s, 2H). ¹³C

NMR (125 MHz, DMSO-d₆, 292 K): δ 166.2, 156.3, 151.5, 151.4, 145.1, 144.9, 142.2, 139.9, 125.9, 122.8, 120.8. ESI-MS: *m/z* 689.0010, [L²Cu]⁺; 652.8796, [L²Cu₂(ClO₄)]⁺. IR (KBr, cm⁻¹): ν(ClO₄⁻); 1083. UV-Vis [CH₃CN; λ_{max}, nm (ε, dm³ mol⁻¹ cm⁻¹)]: 291 (sh), 302 (sh), 335 (9.05 × 10⁴), 348 (8.35 × 10⁴). Anal. Calcd. for C₂₂H₁₄N₆O₈S₂Cl₂Cu₂: C, 35.21; H, 1.88; N, 11.21. Found: C, 35.0; H, 1.89; N, 11.28.



Scheme S9 Synthesis of compound **6A**.

X-Ray Data Collection and Refinement

Single-crystal X-ray studies were performed on a CCD Bruker SMART APEX diffractometer equipped with an Oxford Instruments low-temperature attachment. Data were collected at 100(2) K using graphite-monochromated Mo-Kα radiation ($\lambda_{\alpha} = 0.71073 \text{ \AA}$). The frames were integrated in the Bruker SAINT software package,¹⁰ and the data were corrected for Lorentz and polarization effects. An absorption correction¹¹ was applied. Structures were solved and refined with the SHELX suite of programs¹² as implemented in X-seed.¹³ Hydrogen atoms of the ligands, unless mentioned otherwise, were included in the final stages of the refinement and were refined with a typical riding model. Some of the lattice solvent molecules of complex **4** cannot be modelled satisfactorily due to the presence of severe disorders. Therefore, the Olex-2 mask program has been performed to discard those disordered solvents molecules and gave electron densities of 29.75. This can be tentatively assigned as 1 H₂O and 1 CH₃CN. The crystallographic figures have been generated using Diamond 3 software¹⁴ (50% probability thermal ellipsoids). CCDC files 1518828 (**1**), 907052 (**3A**), 907053 (**4**) 907054 (**5A**), 907055 (**6**) and 907056 (**6A**) contain the supplementary crystallographic data for this paper. These data can be obtained free of charge from the Cambridge Crystallographic Data Centre via www.ccdc.cam.ac.uk/data_request/cif. Pertinent crystallographic data and relevant metrical parameters for compounds **1**, **3A**, **4**, **5A**, **6** and **6A** are summarized in Table **S1–S7**.

Supporting Information

	1	3A 4CH₃CN	4 CH₃CN
Empirical formula	C ₁₄ H ₁₁ BF ₄ MoN ₄ O ₂	C ₃₄ H ₃₂ Cl ₂ N ₁₀ O ₁₂ Ru ₂ S ₂	C ₃₂ H ₁₉ F ₆ N ₉ O ₁₀ Ru ₂ S ₂
Formula Weight	450.02	1109.85	1069.82
Crystal System	Orthorhombic	Monoclinic	Monoclinic
Space Group	<i>Pbcn</i>	<i>P21/n</i>	<i>P121/n1</i>
a (Å)	17.981(6)	12.3747(12)	14.5183(16)
b (Å)	9.755(3)	17.9206(19)	13.3559(15)
c (Å)	18.506(6)	19.028(2)	22.198(2)
α (deg)	90.00	90.00	90.00
β (deg)	90.00	91.200(2)	103.368(2)
γ (deg)	90.00	90.00	90.00
V (Å ³)	3246.3(18)	4218.7(8)	4187.6(8)
Z	8	4	4
ρ _{calcd.} (g cm ⁻³)	1.842	1.747	1.697
μ (mm ⁻¹)	0.868	1.014	0.911
F(000)	1776	2224	2112
Reflections			
Collected	27924	27924	27344
Independent	10396	10396	7739
Observed [I > 2σ (I)]	27344	6936	5056
No. of variables	551	544	551
GOF	1.090	1.001	0.951
R _{int}	0.0720	0.0737	0.0864
Final R indices	R1 = 0.0642	R1 = 0.0579	R1 = 0.0603
[I > 2σ(I)] ^a	wR2 = 0.1329	wR2 = 0.1104	wR2 = 0.1359
R indices (all data) ^a	R1 = 0.1007	R1 = 0.0986	R1 = 0.0954
	wR2 = 0.1497	wR2 = 0.1263	wR2 = 0.1501
	5A	6 CH₃CN	6A
Empirical formula	C ₁₃ H ₁₀ BF ₄ N ₃ O ₂ RhS	C ₂₆ H ₁₉ Cl ₂ Cu ₂ N ₉ O ₈	C ₁₁ H ₇ ClCuN ₃ O ₄ S
Formula Weight	462.02	783.48	376.25
Crystal System	Monoclinic	Monoclinic	Monoclinic
Space Group	<i>P21/n</i>	<i>P21/n</i>	<i>P21/n</i>
a (Å)	9.8778(15)	8.8107(5)	7.0405(10)
b (Å)	13.411(2)	13.3646(8)	13.4755(18)
c (Å)	11.4697(19)	23.9099(15)	13.4023(18)
α (deg)	90.00	90.00	90.00
β (deg)	98.784(4)	97.5930(10)	101.378(2)
γ (deg)	90.00	90.00	90.00
V (Å ³)	1501.6(4)	2790.7(3)	1246.5(3)
Z	4	4	4
ρ _{calcd.} (g cm ⁻³)	2.044	1.865	2.005
μ (mm ⁻¹)	1.336	1.786	2.153
F(000)	908	1576	752
Reflections			
Collected	8569	14718	7938
Independent	3063	5160	3078
Observed [I > 2σ (I)]	1973	4226	2272
No. of variables	210	425	190
GOF	0.993	1.082	1.065
R _{int}	0.0802	0.0347	0.0694
Final R indices	R1 = 0.0613	R1 = 0.0420	R1 = 0.0456
[I > 2σ(I)] ^a	wR2 = 0.1258	wR2 = 0.1042	wR2 = 0.1129
R indices (all data) ^a	R1 = 0.1049	R1 = 0.0520	R1 = 0.0733
	wR2 = 0.1424	wR2 = 1.082	wR2 = 1.065

^aR₁ = Σ ||F_o - |F_c|| / Σ |F_o| with F_o² > 2σ(F_o²). wR₂ = [Σw(|F_o²| - |F_c²|)² / Σ |F_o²|²]^{1/2}

Table S2 Relevant Metrical Parameters for 1 .			
Bond Lengths (Å)			
Mo1–Mo1'	2.1155(9)	Mo1–O1	2.075(4)
Mo1–O2	2.119(4)	Mo1–N1	2.174(4)
Mo1–N2	2.233(4)	Mo1–N3	2.466(5)
Bond Angles (°)			
O1–Mo1–Mo1'	92.92(10)	O1–Mo1–O2'	86.37(15)
N1–Mo1'–N3'	94.37(17)	N2–Mo1–N3	69.18(17)
Mo1–Mo1'–N3'	159.23(12)	O2–Mo1'–N3'	83.18(16)
N1–Mo1'–N2'	93.70(16)	O1–Mo1–N3	106.04(16)
Mo1–Mo1'–N2'	91.35(12)	O2–Mo1'–N2'	89.66(15)
O2–Mo1'–N1	174.85(16)	O1–Mo1–N2	174.16(15)
O1–Mo1–N1'	89.97(16)	Mo1–Mo1'–N1	94.04(13)
Mo1–Mo1'–O2	89.77(10)		

Table S3 Relevant Metrical Parameters for 3A .			
Bond Lengths (Å)			
Ru1–N5	2.047(4)	Ru1–O1	2.059(3)
Ru1–N1	2.065(4)	Ru1–O3	2.089(3)
Ru1–Ru2	2.2906(5)	Ru1–N6	2.293(4)
Ru2–N2	2.050(4)	Ru2–O4	2.056(3)
Ru2–N4	2.074(4)	Ru2–O2	2.080(3)
Ru2–N3	2.246(4)		
Bond Angles (°)			
N5–Ru1–O1	179.62(15)	N5–Ru1–N1	89.24(14)
O1–Ru1–N1	90.41(13)	N5–Ru1–O3	90.73(13)
O1–Ru1–O3	89.62(12)	N1–Ru1–O3	178.37(13)
N5–Ru1–Ru2	90.19(10)	O1–Ru1–Ru2	89.97(9)
N1–Ru1–Ru2	91.06(11)	O3–Ru1–Ru2	87.31(8)
N5–Ru1–N6	76.23(14)	O1–Ru1–N6	103.64(12)
N1–Ru1–N6	93.95(14)	O3–Ru1–N6	87.63(13)
Ru2–Ru1–N6	165.44(9)	N2–Ru2–O4	178.70(14)
N2–Ru2–N4	90.41(15)	O4–Ru2–N4	90.17(14)
N2–Ru2–O2	90.98(14)	O4–Ru2–O2	88.46(13)
N4–Ru2–O2	178.15(13)	N2–Ru2–N3	76.26(15)
O4–Ru2–N3	102.54(14)	N4–Ru2–N3	94.63(14)
O2–Ru2–N3	86.89(12)	N2–Ru2–Ru1	89.98(11)
O4–Ru2–Ru1	91.17(9)	N4–Ru2–Ru1	90.44(11)
O2–Ru2–Ru1	88.34(9)	N3–Ru2–Ru1	165.34(10)

Table S4 Relevant Metrical Parameters for 4 .			
Bond Lengths (Å)			
Ru2–Ru1	2.6714(8)	Ru1–N1	2.186(5)
Ru1–N6	2.142(5)	Ru1–N7	2.174(5)
Ru2–N2	2.133(5)	Ru2–N3	2.137(5)
Ru2–N5	2.192(5)	Ru1–C1	1.853(6)
Ru1–C3	1.866(7)	Ru2–C4	1.862(7)
Ru2–C2	1.876(8)		
Bond Angles (°)			
N2–Ru2–Ru1	85.03(13)	N2–Ru2–N5	85.29(18)
N5–Ru2–Ru1	84.05(13)	N2–Ru2–N3	76.88(19)
C4–Ru2–N2	93.2(2)	C4–Ru2–Ru1	92.6(2)
C4–Ru2–C2	88.3(3)	C4–Ru2–N5	176.4(2)
C2–Ru2–Ru1	97.1(2)	C4–Ru2–N3	94.6(3)
C2–Ru2–N5	93.3(3)	C2–Ru2–N2	177.3(2)
N3–Ru2–Ru1	160.87(15)	C2–Ru2–N3	100.8(2)
N6–Ru1–Ru2	85.31(13)	N3–Ru2–N5	88.3(2)
N6–Ru1–N1	87.50(18)	N6–Ru1–N7	76.42(19)
N7–Ru1–N1	87.46(19)	N7–Ru1–Ru2	160.15(14)
C1–Ru1–Ru2	91.02(18)	N1–Ru1–Ru2	84.01(13)
C1–Ru1–N7	97.4(2)	C1–Ru1–N6	92.5(2)

Supporting Information

C1–Ru1–C3	88.1(3)	C1–Ru1–N1	175.0(2)
C3–Ru1–N1	91.9(2)	C3–Ru1–N7	103.8(2)
C3–Ru1–N6	179.3(2)	C3–Ru1–Ru2	94.4(2)
Table S5 Relevant Metrical Parameters for 5A .			
Bond Lengths (Å)			
Rh1–N2	2.010(6)	Rh1–O1	2.037(5)
Rh1–O2'	2.037(5)	Rh1'–N1	2.041(6)
Rh1–N3	2.292(6)	Rh1–Rh1'	2.4202(12)
O2–Rh1'	2.037(5)		
Bond Angles (°)			
N2–Rh1–O1	90.9(2)	N2–Rh1–O2'	90.4(2)
O1–Rh1–O2'	175.55(19)	N2–Rh1–N1'	176.7(2)
O1–Rh1–N1'	91.0(2)	O2–Rh1'–N1	87.5(2)
N2–Rh1–N3	78.3(2)	O1–Rh1–N3	92.2(2)
O2'–Rh1–N3	92.2(2)	N1'–Rh1–N3	104.3(2)
N2–Rh1–Rh1'	89.00(17)	O1–Rh1–Rh1'	87.38(14)
O2–Rh1'–Rh1	88.37(15)	N1'–Rh1–Rh1'	88.41(17)
N3–Rh1–Rh1'	167.31(16)		
Table S6 Relevant Metrical Parameters for 6 .			
Bond Lengths (Å)			
Cu1–N1	1.947(3)	Cu1–N6	1.985(3)
Cu1–N7	2.168(3)	Cu1–Cu2	2.6199(5)
Cu2–N1S	1.966(3)	Cu2–N5	2.016(3)
Cu2–N2	2.029(3)	Cu2–N3	2.089(3)
Bond Angles (°)			
N1–Cu1–N6	162.47(11)	N1–Cu1–N7	114.58(10)
N6–Cu1–N7	80.08(10)	N1–Cu1–Cu2	87.43(8)
N6–Cu1–Cu2	82.77(8)	N7–Cu1–Cu2	150.16(7)
N1S–Cu2–N5	110.85(11)	N1S–Cu2–N2	110.49(11)
N5–Cu2–N2	135.21(10)	N1S–Cu2–N3	103.64(11)
N5–Cu2–N3	105.98(10)	N2–Cu2–N3	80.05(10)
N1S–Cu2–Cu1	84.17(9)	N5–Cu2–Cu1	83.75(8)
N2–Cu2–Cu1	84.02(7)	N3–Cu2–Cu1	163.89(7)
Table S7 Relevant Metrical Parameters for 6A .			
Bond Lengths (Å)			
Cu1–N1'	1.953(3)	Cu1–N2	1.981(3)
Cu1–N3	2.249(3)	Cu1–Cu1'	2.6468(9)
Cu1–O1	2.395(3)		
Bond Angles (°)			
N1'–Cu1–N2	163.26(12)	N1'–Cu1–N3	108.28(12)
N2–Cu1–N3	80.27(12)	N2–Cu1–O1	106.86(11)
N1'–Cu1–O1	86.24(12)	N3–Cu1–O1	99.82(11)
N1'–Cu1–Cu1'	85.48(9)	N2–Cu1–Cu1'	84.16(9)
N3–Cu1–Cu1'	163.46(9)	O1–Cu1–Cu1'	89.98(8)

Table S8 Chemical shift values for H_a protons of (L¹, L²) and complexes **1**, **2**, **4**, **5**, **5A**, **6**, **6A**.

L ¹ (9.19)		L ² (9.13)
<i>cis</i>	<i>trans</i>	<i>trans</i>
1 (7.70)	5 (9.12)	5A (9.04)
2 (7.79)	6 (9.11)	6A (9.04)
4 (7.74)		

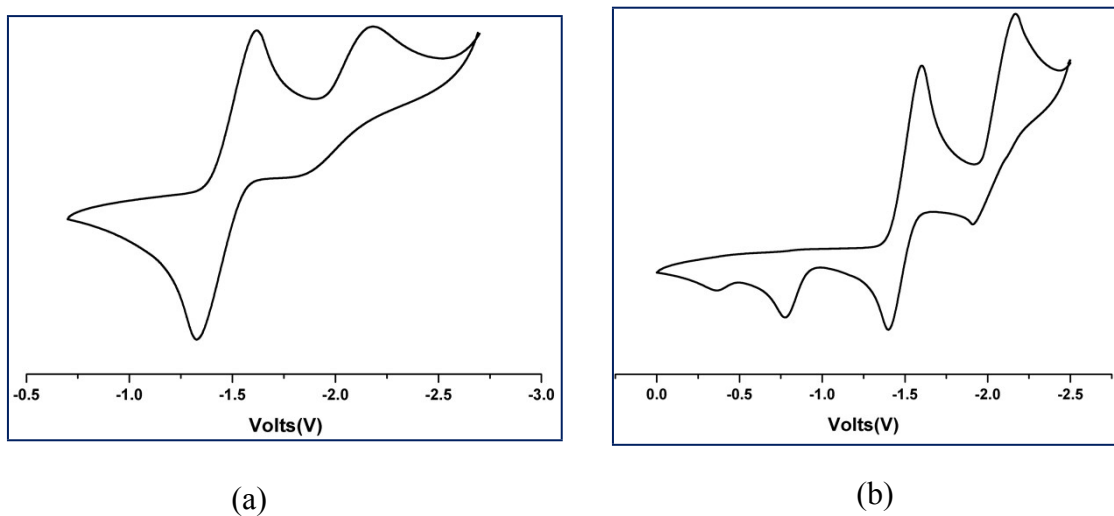


Fig. S1 Cyclic voltammetry of (a) L^1 and (b) L^2 in acetonitrile with TBAP as supporting electrolyte.

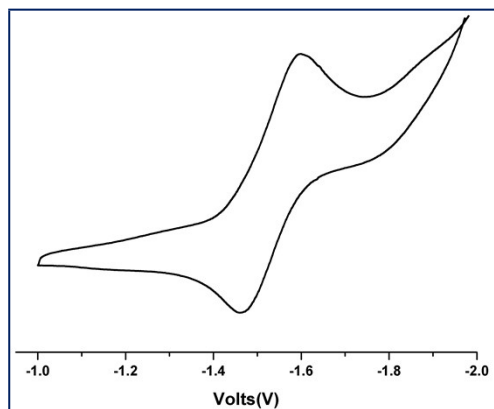


Fig. S2 Cyclic voltammetry of **6A** in acetonitrile with $TBAPF_6$ as supporting electrolyte.

UV–Visible Absorption Spectra of Compounds

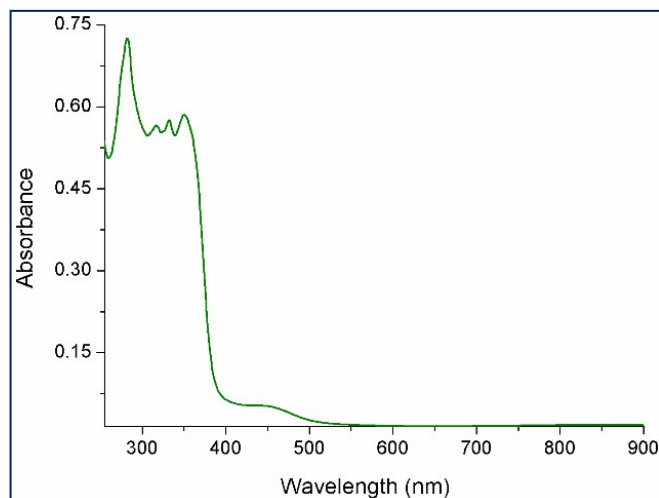


Fig. S3 UV–visible absorption spectrum of **1**.

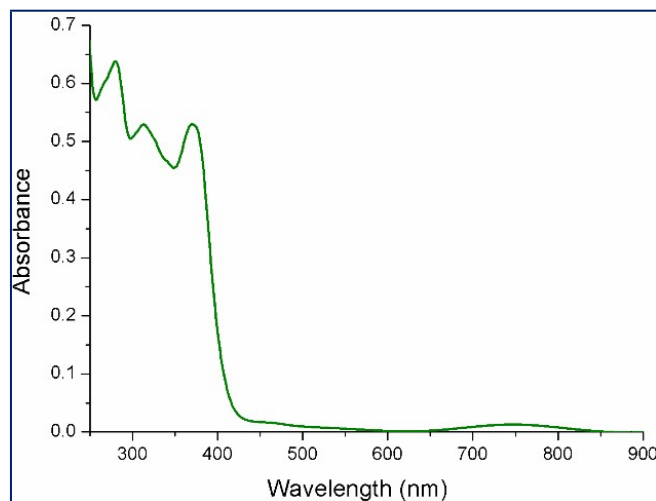


Fig. S4 UV–visible absorption spectrum of **2**.

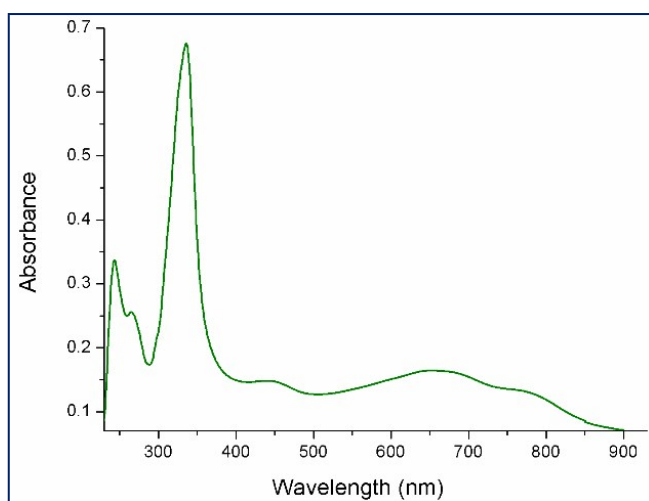


Fig. S5 UV–visible absorption spectrum of **3**.

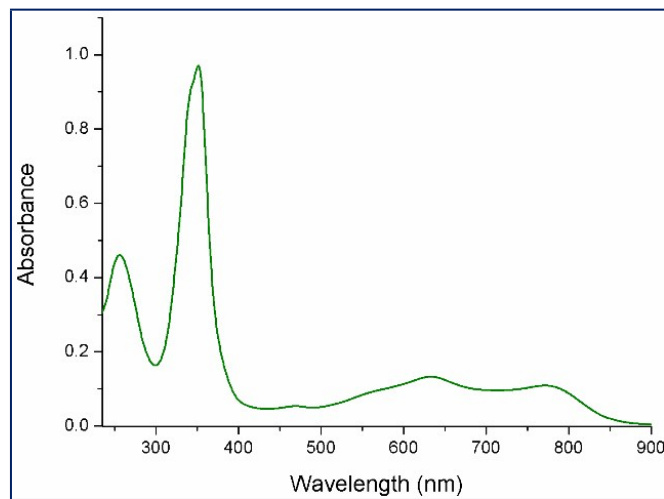


Fig. S6 UV–visible absorption spectrum of **3A**.

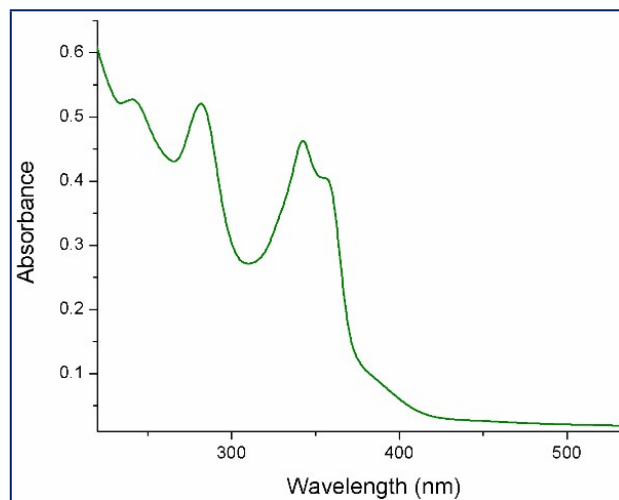


Fig. S7 UV–visible absorption spectrum of **4**.

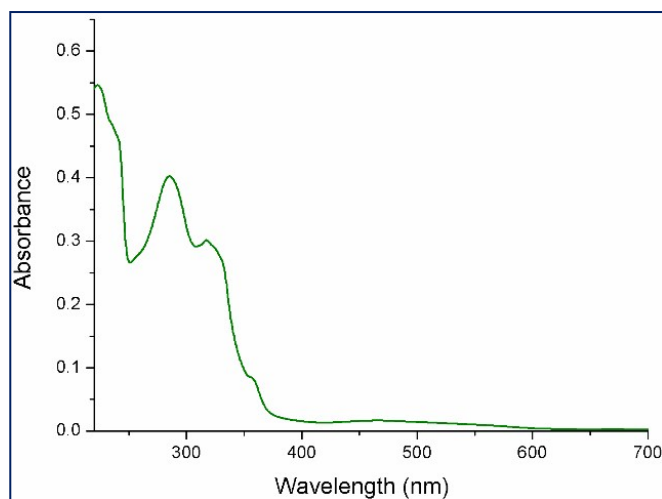


Fig. S8 UV–visible absorption spectrum of **5**.

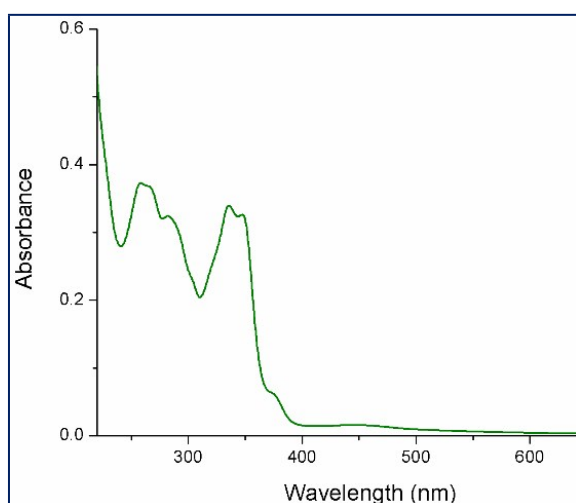


Fig. S9 UV–visible absorption spectrum of **5A**.

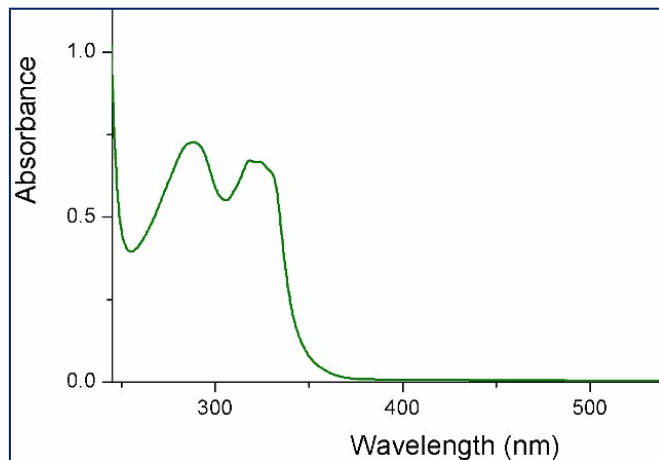


Fig. S10 UV-visible absorption spectrum of **6**.

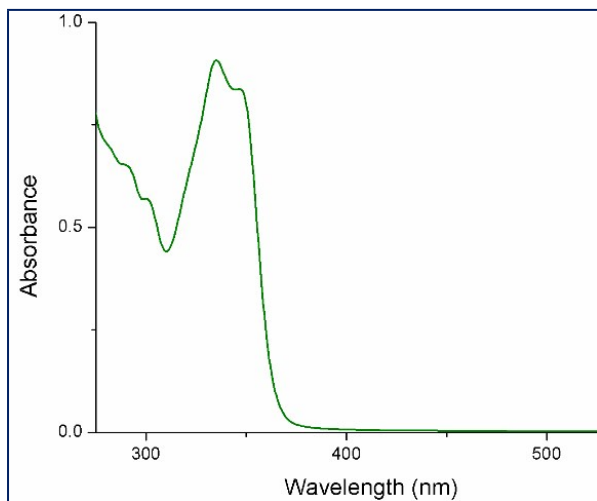


Fig. S11 UV-visible absorption spectrum of **6A**.

Supporting Information

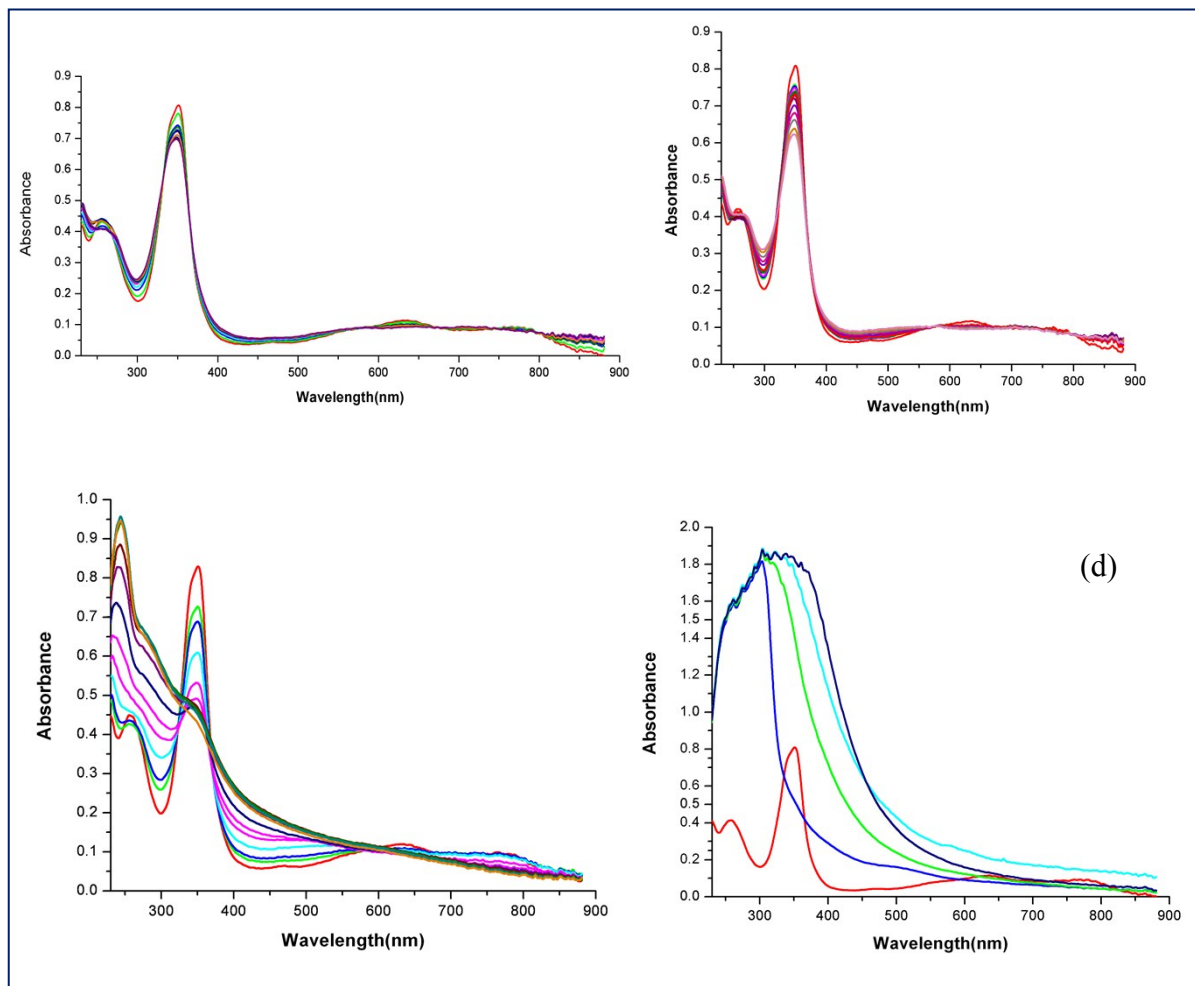


Fig. S12 UV-vis changes monitored (with time) at four potentials (a) -0.17 V (b) -0.57 V (c) -1.17 V and (d) -1.62 V for compound **3A**.

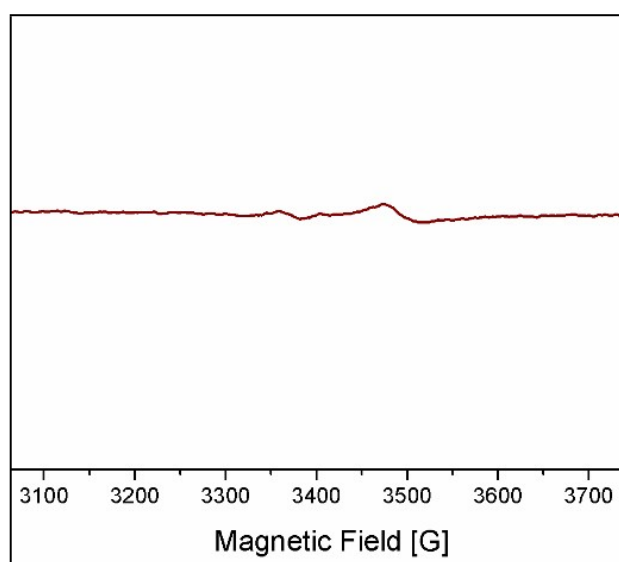
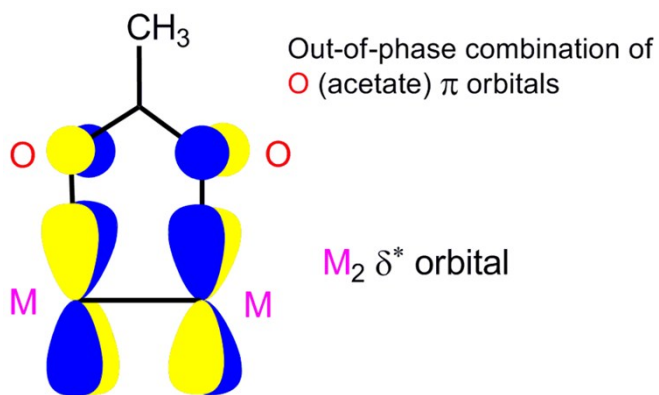


Fig. S13 EPR spectrum for **1** in frozen acetonitrile at 120 K.



Scheme S10 Interaction between $M_2 \delta^*$ orbital and acetate π^* orbital.

Theoretical Study

Calculations were performed using density functional theory (DFT) with Becke's three parameter hybrid exchange functional¹⁵ and the Lee–Yang–Parr correlation functional (B3LYP).¹⁶ Atomic coordinates of the metal–ligand complexes were taken from the single-crystal X–ray structures. The double– ζ basis set of Hay and Wadt (LanL2DZ) with a small core (1s2s2p3s3p3d) effective core potential (ECP)¹⁷ was used for the Mo, Ru, Rh and Cu. The ligand atoms H, C, N and O atoms were described using the 6–31G(d,p) basis sets, and 6–31G+(2d) basis sets for S atom was employed. All calculations were performed with the Gaussian 09 (G09)¹⁸ suite of programs. Gaussview 5 was used for generating the orbital plots.¹⁹ Percentage compositions of the molecular orbitals were calculated from the Gaussian output files using *AOMix* program.²⁰

References

- 1 (a) F. A. Cotton, Z. C. Mester and T. R. Webb, *Acta Cryst.*, 1974, **B30**, 2768; (b) A. B. Brignole and F. A. Coton, *Inorg. Synth.*, 1972, **13**, 87; (c) D. Lawton and R. Mason, *J. Am. Chem. Soc.*, 1965, **87**, 921.
- 2 (a) W. Clegg, G. Pimblett and C. D. Garner, *Polyhedron*, 1986, **5**, 31; (b) G. Pimblett, C. D. Garner and W. Clegg, *J. Chem. Soc., Dalton Trans.*, 1986, 1257; (c) F. A. Cotton, A. H. Reid and W. Schwotzer, *Inorg. Chem.*, 1985, **24**, 3965.
- 3 (a) F. A. Cotton and K. J. Wieinger, *Inorg. Synth.*, 1992, **29**, 134; (b) F. A. Cotton, J. L. Eglin and K. J. Wiesinger, *Inorg. Chim. Acta.*, 1992, **195**, 11; (c) F. A. Cotton and K. J.

Supporting Information

Wiesinger, *Inorg. Chem.*, 1991, **30**, 871; (d) J. Telser and R. S. Drago, *Inorg. Chem.*, 1984, **23**, 1798.

- 4 D. S. Martin, R. A. Newman and I. M. Vlasnik, *Inorg. Chem.*, 1980, **19**, 3404.
- 5 W. J. Klemperer and B. Zhong, *Inorg. Chem.*, 1993, **32**, 5821.
- 6 G. A. Rempel, P. Legzdins, H. Smith and G. Wilkinson, *Inorg. Synth.*, 1972, **13**, 90.
- 7 G. Pimblett, C. D. Garner and W. Clegg, *J. Chem. Soc., Dalton Trans.*, 1986, 1257.
- 8 G. J. Kubas, *Inorg. Synth.*, 1979, **19**, 90.
- 9 (a) K. V. Reddy, K. Mogilaiah and B. Sreenivasulu, *J. Ind. Chem. Soc.*, 1986, **63**, 443; (b) R. P. Thummel, F. Lefoulon, D. Cantu and R. J. Mahadevan, *J. Org. Chem.*, 1984, **49**, 2208; (c) T. C. Majewicz and P. Caluwe, *J. Org. Chem.*, 1974, **39**, 720; (d) E. M. Hawes and D. G. Wibberley, *J. Chem. Soc.*, 1966, 315; (e) D. L. Ashford, C. R. K. Glasson, M. R. Norris, J. J. Concepcion, S. Keinan, M. K. Brennaman, J. L. Templeton and T. J. Meyer, *Inorg. Chem.*, 2014, **53**, 5637.
- 10 SAINT+ Software for CCD diffractometers; Bruker AXS: Madison, WI, 2000.
- 11 G. M. Sheldrick, *SADABS* Program for Correction of Area Detector Data; University of Göttingen: Göttingen, Germany, 1999.
- 12 (a) *SHELXTL* Package v. 6.10; Bruker AXS: Madison, WI, 2000; (b) G. M. Sheldrick, *SHELXS-86* and *SHELXL-97*; University of Göttingen: Göttingen, Germany, 1997.
- 13 (a) J. L. Atwood and L. J. Barbour, *Cryst. Growth Des.*, 2003, **3**, 3; (b) L. J. Barbour, *J. Supramol. Chem.*, 2001, **1**, 189.
- 14 K. Bradenburg, *Diamond, version 3.1e*; Crystal Impact GbR: Bonn, Germany, 2005.
- 15 R. G. Parr and W. Yang, *Density-Functional Theory of Atoms and Molecules*; Oxford University Press: Oxford, U.K., 1989.
- 16 (a) A. D. Becke, *J. Chem. Phys.*, 1993, **98**, 5648; (b) C. Lee, W. Yang and R. G. Parr, *Phys. Rev. B* 1998, **37**, 785.
- 17 (a) P. J. Hay and W. R. Wadt, *J. Chem. Phys.*, 1985, **82**, 270; (b) W. R. Wadt and P. J. Hay, *J. Chem. Phys.*, 1985, **82**, 284; (c) P. J. Hay and W. R. Wadt, *J. Chem. Phys.*, 1985, **82**, 299.
- 18 M. J. Frisch, G. W. Trucks, H. B. Schlegel, G. E. Scuseria, M. A. Robb, J. R. Cheeseman, G. Scalmani, V. Barone, B. Mennucci, G. A. Petersson, H. Nakatsuji, M. Caricato, X. Li, H. P. Hratchian, A. F. Izmaylov, J. Bloino, G. Zheng, J. L. Sonnenberg, M. Hada, M. Ehara, K. Toyota, R. Fukuda, J. Hasegawa, M. Ishida, T. Nakajima, Y. Honda, O. Kitao, H. Nakai, T. Vreven, J. A. Montgomery Jr., J. E. Peralta, F. Ogliaro, M. Bearpark, J. J. Heyd, E. Brothers, K. N. Kudin, V. N. Staroverov, R. Kobayashi, J. Normand, K.

Supporting Information

Raghavachari, A. Rendell, J. C. Burant, S. S. Iyengar, J. Tomasi, M. Cossi, N. Rega, J. M. Millam, M. Klene, J. E. Knox, J. B. Cross, V. Bakken, C. Adamo, J. Jaramillo, R. Gomperts, R. E. Stratmann, O. Yazyev, A. J. Austin, R. Cammi, C. Pomelli, J. W. Ochterski, R. L. Martin, K. Morokuma, V. G. Zakrzewski, G. A. Voth, P. Salvador, J. J. Dannenberg, S. Dapprich, A. D. Daniels, O. Farkas, J. B. Foresman, J. V. Ortiz, J. Cioslowski, D. J. Fox, *Gaussian 09, Revision C.01*; Gaussian, Inc., Wallingford, CT, **2009**.

19 GaussView, **Version 5**, R. Dennington, T. Keith and J. Millam, *Semicem Inc.*, Shawnee Mission, KS, 2009.

20 (a) S. I. Gorelsky, *AOMix: Program for Molecular Orbital Analysis*; York University: Toronto, 1997, <http://www.sg-chem.net/>; (b) S. I. Gorelsky and A. B. P. Lever, *J. Organomet. Chem.* 2001, **635**, 187.